J. Phys.: Condens. Matter **11** (1999) 6595–6604. Printed in the UK PII: S0953-8984(99)03121-5

Mechanism of photoluminescence of Si nanocrystals in SiO_2 fabricated by ion implantation: the role of interactions of nanocrystals and oxygen

Tsutomu Shimizu-Iwayama†§, David E Hole‡ and Ian W Boyd†

† Department of Electronic and Electrical Engineering, University College London, Torrington Place, London WC1E 7JE, UK

‡ School of Engineering, University of Sussex, Falmer, Brighton BN1 9QH, UK

E-mail: t.iwayama@ee.ucl.ac.uk and tiwayama@auecc.aichi-edu.ac.jp

Received 31 March 1999

Abstract. A possible mechanism for the photoemission from Si nanocrystals in an amorphous SiO_2 matrix fabricated by ion implantation is reported. We have measured the implantation dose and the temperature dependence as well as the oxidation effect of the photoluminescence behaviour of Si nanocrystals in SiO_2 layers fabricated by ion implantation and a subsequent annealing step. After annealing, a photoluminescence band, peaking just below 1.7 eV was observed. The peak energy of the photoluminescence was found to be affected by the dose of implanted Si ions and the temperature during ion implantation, but to be independent of annealing time and excitation photon energy. We also present experimental results of an oxidation-induced continuous peak energy shift of the photoluminescence peak up to around 1.8 eV. This peak energy, however, was found to return to its previous position with re-annealing. These results indicate that whilst the excitation photons are absorbed by Si nanocrystals, the emission is not simply due to electron–hole recombination inside the Si nanocrystals, but is related to the presence of defects, most likely located at the interface between the Si nanocrystals and the SiO_2, for which the characteristic energy levels are affected by cluster–cluster interactions or the roughness of the interface.

1. Introduction

In the past decade, there has been considerable interest in semiconductor nanostructures, especially porous Si [1, 2] and Si nanocrystals [3–5] because of their potential applications toward Si-based optoelectronic devices. Si nanocrystals have been fabricated by a variety of methods and include such techniques as co-sputtering, chemical vapour deposition, molecular beam epitaxy, gas evaporation, laser ablation and so on. Nanometre-sized crystallites exhibit unique electrical, optical, magnetic and thermal properties which are not observed in bulk materials. Although a considerable amount of research has been performed by many researchers world wide, the mechanism responsible for photoluminescence from these Si nanostructures is still unclear.

Utilization of porous Si in optoelectronic devices is doubtful because of its method of fabrication and structural fragility. However, one of the most promising approaches to producing Si nanocrystals, compatible with conventional microelectronic processing, may be by ion implantation. This technique has the advantage that a given number of ions can be placed

§ Corresponding author. Permanent address: Department of Materials Science, Aichi University of Education, Igaya-cho, Kariya-shi, Aichi 448-8542, Japan.

0953-8984/99/346595+10$30.00 © 1999 IOP Publishing Ltd

at a controlled depth and distribution by changing the ion doses and acceleration energies [6, 7]. Ion beam synthesis of Si nanocrystals is a potential candidate for manufacturing chemically stable and pure Si nanocrystals, not only for fundamental research, but also for applications in monolithically integrated Si-based optoelectronic devices.

The present authors have carried out a series of studies on the structural and the optical properties of high energy (1 MeV) Si-implanted silica glasses [8–10] and thermally grown oxide films on Si wafers [11–13]. We have shown that these specimens exhibit two luminescence bands in the visible range. One band is peaked around 2.0 eV, is observed in as-implanted specimens and those annealed around 600 °C, and can be attributed to excess Si defects. The other peaks around 1.7 eV and is observed only after annealing at higher temperatures, and can be attributed to Si nanocrystals.

After our first reports [8], many papers [14–21] have appeared concerning the 1.7 eV luminescence in samples prepared employing the same technique of Si ion implantation into SiO_2 and subsequent high temperature annealing. More recently, a dose (implanted excess Si concentration) dependent photoluminescence peak energy shift has also been reported by the present authors [22]. Although the 1.7 eV luminescence is evidently related to implanted Si nanocrystals formed by decomposition of the SiO_x phase with high temperature annealing, the detailed mechanism of the luminescence is not yet clear. The properties of the 1.7 eV luminescence band are similar in many respects to those of other Si nanostructures, and it is likely that the same mechanisms are responsible for the photoluminescence from these materials.

The photoluminescence arising from implanted Si nanocrystals in SiO_2 has been attributed by some investigations to quantum confinement [14, 15], while others have concluded that surface states present in the interfacial layer between the Si nanocrystals and the surrounding oxide matrix play an important role in the emission process [9, 16]. More recently, oxidation effects on photoluminescence from Si nanocrystals fabricated by laser ablation have been reported [23]. This article extends our findings by reporting a wider range of dose and implantation temperature dependencies and oxidation effects on the photoluminescence and discussing a detailed mechanism for the photoemission and tuning of the photoluminescence of the Si nanocrystals formed in SiO_2 by ion implantation, annealing and oxidation steps.

2. Experiment

The samples used were prepared by implanting Si^+ ions into oxidized Si epitaxial layers (10 Ω cm, 10 μm) grown on p^+-type Si wafers with a resistance of around 0.01 Ω cm (oxide thickness of around 600 nm). The Si ions were introduced by a Whickham ion implanter at an acceleration energy of 180 keV to doses ranging from 1.0×10^{16} to 2.0×10^{17} ions cm^{-2} (corresponding to a peak excess Si concentration ranging from 1 to 15%) with a beam current of 570 μA (current density of about 28.5 μA cm^{-2}). The expected depth profiles of the implanted Si atoms in the thermal oxide layers on the Si wafers were estimated using SRIM (the stopping and range of ions in matter) [24] and found to be distributed in near Gaussian profiles peaked around a depth of 270 nm from the surface, similar to that previously measured by Rutherford backscattering spectroscopy [25]. All the implantations were performed with the thermal oxide films kept either at room temperature or at 500 °C.

The implanted samples were subsequently annealed at 1050 °C in a flowing N_2 atmosphere for several hours to induce precipitation and the formation of Si nanocrystals. Some of the samples were then oxidized at 1000 °C in a flowing O_2 atmosphere for up to 90 minutes, and then re-annealed at 1050 °C in a flowing N_2 atmosphere for 1 hour. Conventional room

temperature photoluminescence spectra were measured at various stages of the processing. An Ar-ion laser (2.41 eV or 2.54 eV) was used as the excitation source and the luminescence was detected by a cooled photomultiplier tube, employing the photon counting technique.

3. Results

The photoluminescence spectra of samples annealed at 1050 °C for 8 hours in N_2 are shown in figure 1. The dose dependencies of the photoluminescence peak energy and the intensity are shown in figure 2. The 2.54 eV laser line was used as the excitation source to obtain these spectra and ion implantation was performed at room temperature unless indicated otherwise. It is clear from the figures that the peak energies of the photoluminescence spectra are strongly affected by the dose of implanted Si ions in the high dose range. These peak energies are close to 1.7 eV in the samples with lower doses (below 5×10^{16} ions cm^{-2}), but are shifted to lower energies with increasing dose. The intensity of the luminescence grows and then decreases as

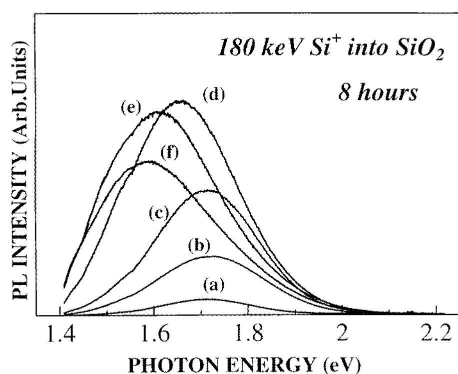

Figure 1. Photoluminescence spectra of 180 keV Si implanted 600 nm thermal oxide films at room temperature to doses of (a) 1×10^{16}, (b) 2.5×10^{16}, (c) 5×10^{16}, (d) 1×10^{17}, (e) 1.5×10^{17} and (f) 2×10^{17} ions cm^{-2} and excited with a 2.54 eV laser, after annealing at 1050 °C for 8 hours in N_2.

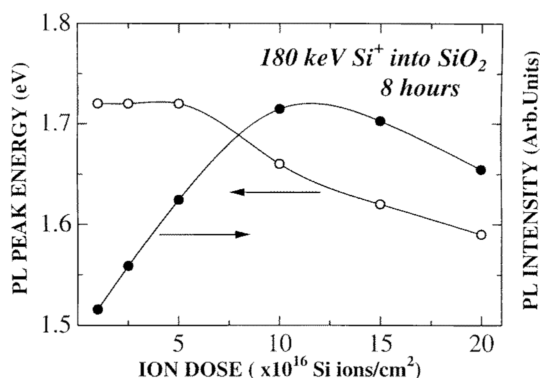

Figure 2. Comparison of the photoluminescence peak energy and the photoluminescence intensity for Si nanocrystals formed by implanting 180 keV Si to different doses, after annealing at 1050 °C for 8 hours in N_2.

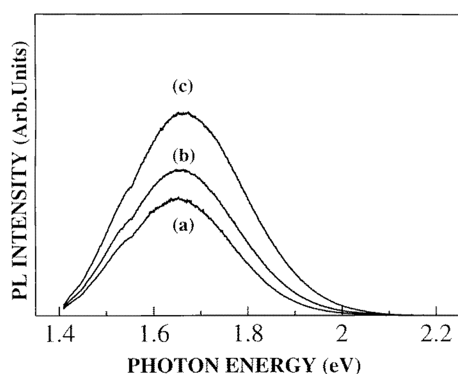

Figure 3. Photoluminescence spectra of samples implanted with 180 keV Si to a dose of 1×10^{17} ions cm^{-2} and excited with a 2.54 eV laser, after annealing at 1050 °C for (a) 2, (b) 4 and (c) 8 hours in N_2.

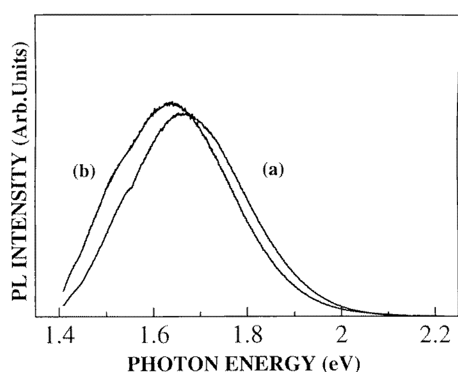

Figure 4. Photoluminescence spectra of samples implanted with 180 keV Si to a dose of 1×10^{17} ions cm^{-2} at (a) room temperature and (b) 500 °C and excited with a 2.54 eV laser, after annealing at 1050 °C for 8 hours in N_2.

the ion dose increases, with the maximum value being obtained at levels of the implanted dose between 1.0×10^{17} and 1.5×10^{17} ions cm^{-2}.

The photoluminescence spectra of samples annealed at 1050 °C for various times in N_2 are shown in figure 3. It is clear from the figure that the luminescence intensity grows as the annealing time increases and also that the peak energies of the spectra are almost independent of annealing time. It is noted that the luminescence intensity grows and then almost saturates with annealing for 8 hours at 1050 °C in all specimens used in the present experiments. Luminescence spectra were also generated using the 2.41 eV excitation laser line. The peak luminescence energies were found to be independent of excitation energy and the only effect of the lower excitation energy was a decrease in the luminescence intensity.

The photoluminescence spectra of samples implanted with a dose of 1.0×10^{17} ions cm^{-2} at room temperature and at 500 °C after an annealing step at 1050 °C for 8 hours in N_2 are shown in figure 4. It is clear from the figure that the peak energies of the spectra are also affected, albeit slightly, by the temperature used during Si ion implantation. The peak energy is reduced by about 0.03 eV for the increased ion implantation temperature even though the

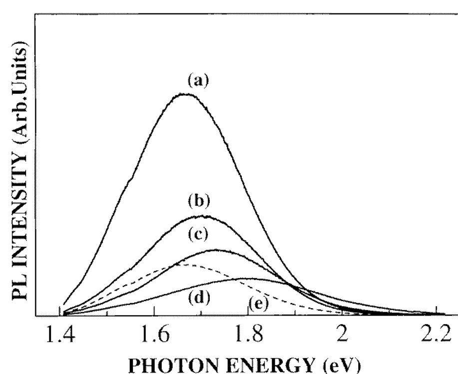

Figure 5. Photoluminescence spectra of samples implanted with 180 keV Si to a dose of 1×10^{17} ions cm^{-2} and excited with a 2.54 eV laser, (a) after annealing at 1050 °C for 8 hours in N_2 and subsequent annealing at 1000 °C for (b) 30, (c) 60 and (d) 90 min in O_2, and (e) re-annealing at 1050 °C in N_2 for 1 hour.

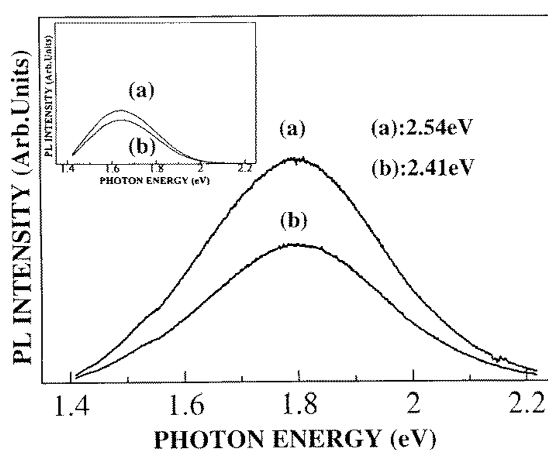

Figure 6. Photoluminescence spectra of sample implanted with 180 keV Si to a dose of 1×10^{17} ions cm^{-2} and excited with (a) 2.54 and (b) 2.41 eV lasers, after annealing at 1050 °C for 8 hours in N_2 and subsequent annealing at 1000 °C for 90 min in O_2. The inset shows the results for samples before oxidation.

implanted dose was the same. It is important to note that the peak energies of the luminescence spectra are also found to be independent of the annealing time and excitation energy in the sample implanted at 500 °C.

The photoluminescence spectra of samples implanted to a dose of 1.0×10^{17} ions cm^{-2} at room temperature after annealing at 1050 °C in N_2 for 8 hours, and subsequently annealed at 1000 °C in O_2 for 30, 60 and 90 minutes are shown in figure 5. In the figure, the spectrum of the samples re-annealed at 1050 °C in N_2 for 1 hour is shown as a dashed line. It is clear from the figure that the peak energies continuously shift to higher values up to around 1.8 eV while the top energies extend to 2.2 eV. Moreover, the photoluminescence band width becomes much broader and the peak intensity decreases with increasing oxidation time. It is also clear that the peak energy returns to almost the same energy as observed before oxidation, while the

intensity levels do not recover with re-annealing in N_2. It is noted that similar peak shifts with oxidation and recoveries were observed in samples implanted with other Si doses.

The photoluminescence spectra obtained using both the 2.41 and 2.54 eV excitation lines have been compared for the sample implanted to a dose of 1.0×10^{17} ions cm^{-2} and annealed at 1050 °C in N_2 for 8 hours and then at 1000 °C in O_2 for 90 minutes and are shown in figure 6. The inset shows the results for samples before oxidation. The peak energies of the spectra are clearly not affected by the excitation energy and the only difference is the decrease of luminescence intensity, similar to that observed in the samples before oxidation. Similar experimental results were obtained in all of the oxidation steps investigated.

4. Discussion

It is useful at this stage to review previous experimental results of cross-section high-resolution transmission electron microscopy [13, 26, 27]. We have previously reported that no trace of the formation of crystalline Si is evident in Si-implanted samples before high-temperature heat treatment. After treatment at high temperatures, however, electron micrographs have indicated the presence of Si nanocrystals in an amorphous SiO_2 matrix for samples implanted with 1 MeV Si ions to a dose of 2×10^{17} ions cm^{-2} (peak excess Si concentration of about 8%) around the depth of the projected range of the implanted Si in SiO_2. Moreover, we have also observed an increase in the size of the Si crystallites after extending the annealing time.

The increase in size and also the number of Si nanocrystals when increasing the ion dose for samples implanted with a few hundred keV energy Si ions was confirmed by White *et al* [26]. Brongersma *et al* [27] have also reported that annealing of 35 keV Si-implanted samples in O_2 at 1000 °C after high-temperature annealing without O_2 results in oxidation of the Si nanocrystals in SiO_2. They also showed that the oxidation of the Si nanocrystals starts at the surface and, as time progresses, the oxidation front moves deeper into the film, and the oxidation front is wide and a relatively wide region is oxidizing at the same time. Thus, the size distribution of the Si nanocrystals shifts to smaller sizes due to the oxidation process.

4.1. Implantation dose dependent photoluminescence peak energy shift

Firstly, we discuss the dose dependence of the photoluminescence from the Si nanocrystals. From the experimental results of the dose dependent peak energy shift of the photoluminescence alone, it seems reasonable to assume that the origin of the photoluminescence is due to quantum confinement effects and that the peak shift could be explained by a change in the size of the Si nanocrystals. However, as we mentioned above, the size of the Si nanocrystals depends on both the implantation dose and the annealing time. An important point to note is that the luminescence intensity grows during annealing, without changing the peak energy of the spectra, as shown in figure 3. Since the Si nanocrystals grow as the annealing time increases, the lack of dependence of the peak energy on the annealing time excludes the possibility that the luminescence is simply due to the direct recombination between electrons and holes confined inside the Si nanocrystals. Other groups have suggested that the absorption of photons leads to the generation of electron–hole pairs which are confined within the Si nanocrystals, whilst the emission of photons arises from surface states localized at the interface between the Si nanocrystals and the SiO_2 matrix [28, 29]. However, with these models, we cannot explain our observed dose dependent shift of the photoluminescence.

We have recently proposed an alternative model [22] to explain the peak shift of the photoluminescence. In this model, we consider that the bandgap widening due to the quantum confinement effect plays an essential role in the photo-absorption process and the interface

energy state between the Si nanocrystals and the thin SiO_2 layer, for which the energy levels are affected by cluster–cluster interactions, plays an essential role in the luminescence process. If the Si nanocrystal population is very dense, the nanocrystals interact with each other via the thin intervening oxide and a decrease in the interface energy level should be expected. With larger implanted Si doses, of course, the local concentration of Si atoms before annealing is much higher, and this contributes to an increase in both the size and the number of Si nanocrystals after annealing, as observed by others [26]. However, once the nucleation of Si aggregates occurs by decomposition of SiO_x, a point would be reached where the Si nanocrystals formed would not migrate within the SiO_2 matrix. Below a dose of 5×10^{16} ions cm^{-2}, the peak energy is almost fixed at around 1.7 eV. This energy seems to be the interfacial energy level between the Si nanocrystals and the SiO_2 matrix without any interactions.

Now, we discuss the dose dependent change in photoluminescence intensity. For the case of Si nanocrystals, the luminescence intensity is determined by the number of (optimally sized) Si nanocrystals and/or their luminescence efficiency, if we assume that their absorption cross-section is the same at the excitation energy (2.54 eV). Up to a dose around 1.0×10^{17} ions cm^{-2}, the photoluminescence intensity increases as the dose increases, as shown in figure 2. The number and the growth of the Si nanocrystals are both expected to increase with the dose. Thus the initial intensity increase with implanted Si ion dose, as shown in figure 2, is consistent with the presumption. Above a dose of 1.0×10^{17} ions cm^{-2}, the intensity of the photoluminescence falls as the dose increases. There are several possible reasons for this. Firstly, the band-to-band transition energy of the confined Si nanocrystal system should be smaller than the emission energy with the growth of the Si nanocrystals. Secondly, interactions between the nanocrystals will affect the photoluminescence efficiency. Thirdly, as the size of the Si nanocrystals increases the interface-to-volume ratio decreases. Fourthly, the probability of energy transfer to the interface will decrease, particularly if the nanocrystals include imperfections. In any case we expect that the highest photoluminescence intensity will be observed from the samples when appropriately sized Si nanocrystals have been optimally distributed within the SiO_2 matrix.

4.2. Implantation temperature dependent photoluminescence peak energy shift

Before discussing the implantation temperature dependence of the photoluminescence of the Si nanocrystals, it is noted that the heating of the surface layer by the action of ion implantation is less than 100 °C and therefore far too low to induce any significant changes in our specimens. The effect of implantation dose will be mainly to extend the time the specimens are hot, and since the temperature rise is already too low for anything to happen, will also have no influence.

Now, we discuss the implantation temperature dependence of the photoluminescence. The peak energies are shifted about 0.03 eV to lower energies with increasing implantation temperature from room temperature to 500 °C. Based on the model explained in the previous section, we can explain this shift as follows. In forming the Si nanocrystals in an SiO_2 matrix by high-temperature annealing, diffusion, nucleation and growth (i.e. crystallization) processes are clearly important. The implanted Si ions will initially form SiO_x, or to a lesser extent, Si aggregates. As the present authors have previously reported [9, 11], the initial state of the implanted Si is strongly affected by the substrate temperature during ion implantation. With increasing implantation temperature, the implanted Si ions tend to form small aggregates (less than the typical nanocrystal formed in this study). Annealing at high temperature induces diffusion and nucleation of excess Si atoms, and prolonged annealing induces growth of the Si aggregates. Therefore, samples implanted at 500 °C will contain more nucleation points (Si aggregates), which are formed during the implantation process, than those implanted at room temperature. As a result, a larger number of Si nanocrystals are formed in the SiO_2 matrix

and the average distance between the nanocrystals decreases, such that stronger cluster–cluster interactions via the thin intervening oxide can be expected in the samples implanted at higher temperature.

4.3. Oxidation induced photoluminescence peak energy shift

Finally, we discuss the oxidation-induced peak energy shift of the photoluminescence spectra of the Si nanocrystals. Since the average size of the Si nanocrystals evidently decreases as the oxidation time increases, it seems that the origin of this shift is due to quantum confinement effects, as others have already concluded [27]. An important point to note, however, is that the peak energy returns to its original peak position after re-annealing in N_2. With annealing in O_2, of course, the average size of the Si nanocrystals decreases and the remaining excess Si atoms will oxidize. If we assume that the origin of the peak energy shift is due to quantum confinement and the photoluminescence is simply due to the direct recombination between electrons and holes confined inside the Si nanocrystals, this means that the Si nanocrystals return to their previous size after re-annealing in N_2. It is not easy to understand this annealing-induced recovery in size for samples with such a deficient excess Si concentration and this strongly suggests that other factors affect the shift of the spectra after oxidation.

A photoluminescence peak energy above $\sim$1.7 eV will not be expected with our model as we have already discussed. It seems, therefore, that a change in the interfacial energy states with oxidation could induce the observed change in the photoluminescence peak energy. It is noted that the excitation energy dependence of this photoluminescence band is different to that observed in the as-implanted samples and is not related to the Si nanocrystals *per se* but can be attributed to excess Si defects. The peak energy of the photoluminescence band observed before thermal annealing depends on excitation energy [30], but that observed after oxidation does not, similar to that before oxidation, as shown in figure 6. This indicates that the origin of the photoluminescence is different from that observed before annealing.

It is well known that the luminescence emitted by recombination of the self-trapped excitons in crystalline SiO_2 peaks at 2.8 eV [31–33]. This luminescence is thought to be due to the recombination of an electron on the Si dangling bond and a hole on the O dangling bond, which are generated by the breaking of a Si–O bond [34, 35]. The corresponding luminescence band in amorphous SiO_2 has been shown to peak around 2.3 eV [36]. Moreover, the luminescence band observed around 2.0 eV in Si-implanted SiO_2 before high-temperature annealing, in which the peak energy depends on both the implantation dose and the substrate temperature during implantation, can be attributed to the formation of excess Si defects [9–11]. It is suggested that the peak energy of the luminescence in all these Si–O systems is sensitive to a variety of local disorders which include both structural and bond disorder. The arguments above suggest that the photoluminescence observed above 1.7 eV after oxidation is due to the recombination of electrons and holes at the interface between Si nanocrystals and SiO_2, and the introduction of different oxidation states to those present before oxidation. These new oxidation states seem to be metastable and easily transformed to more stable states by annealing in a non-oxygen ambient. These experimental results indicate that the peak energies of the photoluminescence above 1.7 eV could be strongly affected by the roughness of the interface.

More recently, Patrone *et al* [23] reported oxidation effects on the photoluminescence from Si nanocrystals fabricated by laser ablation. They observed enhancement and the peak shift of the photoluminescence. These results arise from passivation of surface of nanocrystals and reduction of the size, and they have concluded that the observed photoluminescence could be the transition between quantum-confined levels of nanosized silicon crystals. The difference

from our results seems to be arise the difference of the oxidation condition (they oxidized at room temperature) and excitation photon energy (they used 4.8 eV). Again, we would like to stress that the photoluminescence peak energies after oxidation return to their previous position with slightly annealing without oxygen in our study; it is not easy to understand this annealing-induced recovery in size for samples with such a deficient excess Si concentration, and it is not consistent with a simple quantum confinement model. Detailed comparisons of our results with theirs will be made in the near future.

5. Conclusion

We have measured the implantation dose, implantation temperature dependence and the effect of oxidation on the photoluminescence of Si nanocrystals in SiO_2 layers, fabricated by ion implantation and subsequent annealing and oxidation steps. We have found that the peak energy of the photoluminescence was almost independent of the size of the Si nanocrystals if they have an appropriate size (i.e. the band-to-band transition energy of the confined Si system should be smaller than the incident photon energy and larger than the emission photon energy), but strongly affected by the mutual distance of nanocrystals (i.e. their concentration) for the photoemission below 1.7 eV, or the roughness (oxidation state) of the interface for the photoemission above 1.7 eV. This method of fabricating Si nanocrystals, by ion implantation and subsequent high-temperature annealing, is found to be an important technique that enables the isolation and the identification of some factors which affect the peak energy of the photoluminescence spectra. Further studies of the size and distribution of the Si nanocrystals in these Si-implanted SiO_2 layers by cross-section high-resolution transmission electron microscopy and additive experiments, including temperature and excitation power dependence of the photoluminescence, are now in progress.

Acknowledgments

The authors would like to express their gratitude to Professor P D Townsend, University of Sussex for use of the ion implanter and for helpful discussions, and to Mr Makoto Takiyama, Nittetsu Denshi Corporation for supplying the Si wafers with thermal oxide films. This work has been partly supported by the Japan Securities Scholarship Foundation, the Daiwa Anglo-Japanese Foundation, the British Council, the Marubun Foundation, the Yazaki Memorial Foundation for Science and Technology and the Ministry of Education, Science, Sports and Culture, Grant-in-Aid Japan.

References

[1] Canham L T 1990 *Appl. Phys. Lett.* **57** 1046
Cullis A G, Canham L T and Calcott P D 1997 *J. Appl. Phys.* **82** 909
[2] Lehmann V and Gösele U 1991 *Appl. Phys. Lett.* **58** 856
[3] DiMaria D J, Kirtley J R, Pakulis E J, Dong D W, Kuan T S, Pesavento F L, Theis T N and Cutro J A 1984 *J. Appl. Phys.* **56** 401
[4] Furukawa S and Miyasato T 1988 *Japan. J. Appl. Phys.* **27** L2207
[5] Takagi H, Ogawa H, Yamazaki Y, Ishizaki A and Nakagiri T 1990 *Appl. Phys. Lett.* **56** 2379
[6] Ziegler J F 1992 *Ion Implantation Technology* ed J F Ziegler (Amsterdam: North-Holland) p 1
[7] Townsend P D, Chandler P J and Zhang L 1994 *Optical Effects of Ion Implantation* (Cambridge: Cambridge University Press)
[8] Iwayama T S, Ohshima M, Niimi T, Nakao S, Saitoh K, Fujita T and Itoh N 1993 *J. Phys.: Condens. Matter* **5** L375

[9] Iwayama T S, Fujita K, Nakao S, Saitoh K, Fujita T and Itoh N 1994 *J. Appl. Phys.* **75** 7779
[10] Itoh N, Iwayama T S and Fujita T 1994 *J. Non-Cryst. Solids* **179** 194
[11] Iwayama T S, Nakao S and Saitoh K 1994 *Appl. Phys. Lett.* **65** 1814
[12] Iwayama T S, Nakao S, Saitoh K and Itoh N 1994 *J. Phys.: Condens. Matter* **6** L601
[13] Iwayama T S, Terao Y, Kamiya A, Takeda M, Nakao S and Saitoh K 1995 *Nanostruct. Mater.* **5** 307
[14] Atwater H A, Shcheglov K V, Wong S S, Vahala K J, Flagan R C, Brongersma M L and Polman A 1994 *Mater. Res. Soc. Symp. Proc.* vol 316 (Pittsburgh, PA: Materials Research Society) p 409
Min K S, Shcheglov K V, Yang C M, Atwater H A, Brongersma M L and Polman A 1996 *Appl. Phys. Lett.* **69** 2033
[15] Mutti P, Ghislotti G, Bertoni S, Bonoldi L, Cerofolini G F, Meda L, Grilli E and Gruzzi M 1995 *Appl. Phys. Lett.* **66** 851
[16] Zhu J G, White C W, Budai J D, Withrow S P and Chen Y 1995 *Mater. Res. Soc. Symp. Proc.* vol 358 (Pittsburgh, PA: Materials Research Society) p 163
Zhu J G, White C W, Budai J D, Withrow S P and Chen Y 1995 *J. Appl. Phys.* **77** 4386
[17] Komoda T, Kelly J P, Nejim A, Homewood K P, Hemment P L F and Sealy B J 1995 *Mater. Res. Soc. Symp. Proc.* vol 358 (Pittsburgh, PA: Materials Research Society) p 175
[18] Skorupa W, Yankov R A, Tyschenko I E, Fröb H, Böhme T and Leo K 1996 *Appl. Phys. Lett.* **68** 2410
[19] Fischer T, Petrova-Koch V, Shcheglov K, Brandt M S and Koch F 1996 *Thin Solid Films* **275** 100
[20] Guha S, Pace M D, Dunn D N and Singer I L 1997 *Appl. Phys. Lett.* **70** 1207
[21] Song H Z and Bao X M 1997 *Phys. Rev.* B **55** 6988
[22] Iwayama T S, Kurumado N, Hole D E and Townsend P D 1998 *J. Appl. Phys.* **83** 6018
[23] Patrone L, Nelson D, Safarov V, Sentis M and Marine W 1999 *J. Lumin.* **80** 217
[24] Ziegler J F, Biersack J P and Littmark U L 1985 *The Stopping and Range of Ions in Solids* (New York: Pergamon)
[25] Shimizu T, Itoh N and Matsunami N 1988 *J. Appl. Phys.* **64** 3663
[26] White C W, Budai J D, Withrow S P, Zhu J G, Pennycook S J, Zuhr R A, Hembree D M Jr, Henderson D O, Magruder R H, Yacaman M J, Mondragon G and Prawer S 1997 *Nucl. Instrum. Methods* B **127/128** 545
White C W, Budai J D, Withrow S P, Zhu J G, Sonder E, Zuhr R A, Meldrum A, Hembree D M Jr, Henderson D O and Prawer S 1998 *Nucl. Instrum. Methods* B **141** 228
[27] Brongersma M L, Polman A, Min K S, Boer E, Tambo T and Atwater H A 1998 *Appl. Phys. Lett.* **72** 2577
[28] Koch F, Petrova-Koch V and Muschik T 1993 *J. Lumin.* **57** 271
[29] Kanemitsu Y, Ogawa T, Shiraishi K and Takeda K 1993 *Phys. Rev.* B **48** 4883
[30] Iwayama T S, Terao Y, Kamiya A, Takeda M, Nakao S and Saitoh K 1996 *Thin Solid Films* **276** 104
[31] Griscom D L 1979 *Proc. 3rd Int. Frequency Control Symp.* (Washington DC: Electronic Industries Association) p 98
[32] Trukhin A N 1979 *Sov. Phys.–Solid State* **21** 644
[33] Itoh C, Tanimura K, Itoh N and Itoh M 1989 *Phys. Rev.* B **39** 11 183
[34] Shluger A L 1988 *J. Phys. C: Solid State Phys.* **21** L432
[35] Shluger A and Stefanovich E 1990 *Phys. Rev.* B **42** 9664
[36] Itoh N, Tanimura K and Itoh C 1988 *The Physics and Technology of Amorphous* SiO_2 ed R A B Devine (New York: Plenum) p 135